



HAL
open science

Detection of regional scale sea-to-air oxygen emission related to spring bloom near Japan by using in-situ measurements of atmospheric oxygen/nitrogen ratio

H. Yamagishi, Y. Tohjima, H. Mukai, K. Sasaoka

► **To cite this version:**

H. Yamagishi, Y. Tohjima, H. Mukai, K. Sasaoka. Detection of regional scale sea-to-air oxygen emission related to spring bloom near Japan by using in-situ measurements of atmospheric oxygen/nitrogen ratio. *Atmospheric Chemistry and Physics Discussions*, 2008, 8 (1), pp.2225-2248. hal-00303285

HAL Id: hal-00303285

<https://hal.science/hal-00303285>

Submitted on 18 Jun 2008

HAL is a multi-disciplinary open access archive for the deposit and dissemination of scientific research documents, whether they are published or not. The documents may come from teaching and research institutions in France or abroad, or from public or private research centers.

L'archive ouverte pluridisciplinaire **HAL**, est destinée au dépôt et à la diffusion de documents scientifiques de niveau recherche, publiés ou non, émanant des établissements d'enseignement et de recherche français ou étrangers, des laboratoires publics ou privés.

Detection of regional scale sea-to-air oxygen emission related to spring bloom near Japan by using in-situ measurements of atmospheric oxygen/nitrogen ratio

H. Yamagishi¹, Y. Tohjima¹, H. Mukai², and K. Sasaoka³

¹Atmospheric Environmental Division, National Institute for Environmental Studies, Tsukuba, Japan

²Center for Global Environmental Research, National Institute for Environmental Studies, Tsukuba, Japan

³Frontier Research Center for Global Change, Japan Agency for Marine-Earth Science and Technology, Yokohama, Japan

Received: 19 November 2007 – Accepted: 2 January 2008 – Published: 6 February 2008

Correspondence to: H. Yamagishi (yamagishi.hiroaki@nies.go.jp)

Detection of oxygen emission related to spring bloom

H. Yamagishi et al.

Title Page

Abstract

Introduction

Conclusions

References

Tables

Figures

⏪

⏩

◀

▶

Back

Close

Full Screen / Esc

Printer-friendly Version

Interactive Discussion

Abstract

We have been carrying out in-situ monitoring of atmospheric O_2/N_2 ratio at Cape Ochiishi (COI; $43^\circ 10' N$, $145^\circ 30' E$) in the northern part of Japan since March 2005 by using a modified gas chromatography/thermal conductivity detector (GC/TCD). The standard deviation of the O_2/N_2 ratio is estimated to be about ± 14 per meg (≈ 3 ppm) with intervals of 10 min. Thus, the in-situ measurement system has a 1σ precision of ± 6 per meg (≈ 1.2 ppm) for one-hour mean O_2/N_2 ratio. Atmospheric potential oxygen (APO $\approx O_2 + 1.1CO_2$), which is conserved with respect to terrestrial photosynthesis and respiration but reflects changes in air-sea O_2 and CO_2 fluxes, shows large variabilities from April to early July 2005. Distribution of satellite-derived marine primary production indicates occurrences of strong bloom in the Japan Sea in April and in the Okhotsk Sea and the western North Pacific near Hokkaido Island in June. Back trajectory analysis of air masses indicates that high values of APO, which last for several hours or several days, can be attributed to the oxygen emission associated with the spring bloom of active primary production.

1 Introduction

Observation of atmospheric oxygen has been conducted for decades since the development of methods for measuring atmospheric O_2/N_2 ratios (e.g. Keeling, 1988; Bender et al., 1994). Changes in atmospheric O_2 have been applied to resolve the carbon budget, exploiting the nature of the molar $O_2:C$ exchange ratios in fossil fuel combustion (Keeling, 1988) and in land biotic photosynthesis and respiration (Severinghaus, 1995). For oceanic fluxes, exchange of O_2 is much faster than that of CO_2 . It takes only 3 weeks for dissolved oxygen to equilibrate with the atmosphere, whereas it takes about a year for CO_2 because of the different equilibration time scales of various carbonate species (Broecker and Peng, 1982). Therefore, because of the apparent independence of the air-sea exchange of CO_2 and O_2 due to the fast response of O_2

Detection of oxygen emission related to spring bloom

H. Yamagishi et al.

Title Page

Abstract

Introduction

Conclusions

References

Tables

Figures

◀

▶

◀

▶

Back

Close

Full Screen / Esc

Printer-friendly Version

Interactive Discussion

relative to CO₂, seasonal variations in atmospheric oxygen have been used to estimate marine productivity (Keeling and Shertz, 1992; Bender et al., 1996; Balkanski et al., 1999).

Stephens et al. (1998) introduced Atmospheric Potential Oxygen (APO \approx O₂+1.1 CO₂) as a conservative tracer for O₂ and CO₂ exchange related to land biotic photosynthesis and respiration. The concept of APO is similar to the oceanic component of the O₂/N₂ ratio, which has been discussed by Keeling and Shertz (1992). Although spatial and temporal distributions of APO have been revealed through flask sample measurements (Battle et al., 2006; Manning and Keeling, 2006; Tohjima et al., 2005b), there are short-term APO variations that can not be detected from flask sampling. At stations such as Cold Bay, Alaska (CAB: 55° N, 162° E) (Battle et al., 2006) and Cape Ochi-ishi, Hokkaido (COI: 43°10' N, 145°30' E) (Tohjima et al., 2008), plots of APO are scattered, which may be related to variation of O₂ flux from the oceans caused by active marine primary production near the stations.

In-situ measurements at stations can significantly increase the temporal resolution of atmospheric O₂ measurements, leading to new insights into marine productivity and air-sea oxygen flux on even smaller time and space scales. Various techniques have been developed to make in-situ measurements of the atmospheric O₂/N₂ ratio, such as the paramagnetic oxygen analyzer system (Lueker et al., 2003; Manning et al., 1999), the vacuum ultraviolet absorption method (Stephens, 1999; Stephens et al., 2003), and the fuel cell analyzer systems (Stephens et al., 2007 and references therein). Previous studies have revealed that a sampling line for in-situ O₂/N₂ measurements requires careful design to prevent fractionation of O₂ from N₂. Thermal fractionation between O₂ and N₂ can easily occur at various locations, such as the sampling line inlet (Blaine et al., 2006; Stephens et al., 2007; Sturm et al., 2006) and tee junctions (Keeling et al., 2004; Manning, 2001; Stephens et al., 2003).

Tohjima (2000) developed an analytical system for measuring O₂/N₂ ratio by using a gas chromatograph equipped with a thermal conductivity detector (GC/TCD). The GC/TCD method has been used to analyze flask samples collected at monitoring sta-

Detection of oxygen emission related to spring bloom

H. Yamagishi et al.

Title Page

Abstract

Introduction

Conclusions

References

Tables

Figures

◀

▶

◀

▶

Back

Close

Full Screen / Esc

Printer-friendly Version

Interactive Discussion

Detection of oxygen emission related to spring bloom

H. Yamagishi et al.

[Title Page](#)[Abstract](#)[Introduction](#)[Conclusions](#)[References](#)[Tables](#)[Figures](#)[◀](#)[▶](#)[◀](#)[▶](#)[Back](#)[Close](#)[Full Screen / Esc](#)[Printer-friendly Version](#)[Interactive Discussion](#)

tions and cargo ships (Tohjima et al., 2003; Tohjima et al., 2005b) and has the potential to be applied for field-base measurements. In this study, we set up a field-base O_2/N_2 measurement system at COI, which is located at the eastern coast of Hokkaido island in Japan. APO at COI shows large variability especially during spring and summer (Tohjima et al., 2008). To examine the causes of the variability of APO at COI, we have monitored the O_2/N_2 ratio since 17 March 2005. Here, we show the details of the in-situ measurement system and the quality and reliability of the obtained data. We also made analysis of short-term variations (temporal scales of several hours to days) in APO from April to early July 2005 using back trajectory analysis and found that the APO variation can be attributed to the regional-scale oxygen emission resulting from spring bloom in the Japan Sea, the Okhotsk Sea, and the western North Pacific.

2 Methods

2.1 Sampling line

An air intake, which is capped with an inverted stainless steel beaker covered with stainless steel mesh, is placed on the tower at ~ 51 m height above ground level (~ 100 m height above sea level) at COI. Sample air is drawn through 1/4 inch OD, 4.35 mm ID stainless (SUS 316) tubing from the tower to the inside of the station using an oil-free diaphragm pump (model MOA-P108-HB, Gast Mfg. Corp., Benton Harbor, MI, USA) at a rate of ~ 8 L min^{-1} . This fast sample flow rate was chosen to prevent thermal fractionation between O_2 , N_2 , and Ar at the inlet of the sample line (Keeling et al., 1998).

The measurement system requires a 8 mL min^{-1} flow rate, which is one thousandth of the main flow rate of the sample gas. Previous studies have found that the fractionation of O_2 from N_2 occurs at a tee junction when there is a thermal gradient in the tee junction or the flow ratio between the two separated flows is large (Keeling et al., 2004; Manning et al., 1999; Stephens et al., 2003). To separate the sample gas without

Detection of oxygen emission related to spring bloom

H. Yamagishi et al.

Title Page

Abstract

Introduction

Conclusions

References

Tables

Figures

◀

▶

◀

▶

Back

Close

Full Screen / Esc

Printer-friendly Version

Interactive Discussion

fractionation at tee junctions, Stephens et al. (2007) have developed a special tee configuration, in which a thin pick-off tubing extends upstream into a larger O. D. tubing. In our case we inserted a 2-L spherical Pyrex®-glass flask into the main sample flow as a buffer volume for picking up the required small sample gas flow for measurement (see Fig. 1).

After the air sample is drawn from the intake with a 1/4" tubing, it is passed through a 7- μ m-pore-sized filter in a stainless housing and compressed into the spherical flask at a pressure of 0.06 MPa above atmospheric pressure by the diaphragm pump (see Fig. 1 for details of the sample line). The pressure in the spherical flask is adjusted using a back pressure valve. A drain port on the spherical flask removes water condensed from vapor in the air sample. The air sample is then collected from the center of the spherical flask using a 1/16 inch OD, 0.80 mm ID stainless steel tubing (SUS 316) at a continuous flow rate of 8 mL min⁻¹.

After sample collection, the air sample is dried further by passing through an 80-mL Pyrex®-glass trap immersed in an alcohol bath (-80°C). The alcohol bath is cooled using a low temperature freeze trap VA-500F (Taitec Corp., Koshigaya, Japan). Although a large temperature gradient in the glass trap leads to large gradients of O₂ and N₂ between the bottom and top of the trap, the constant flow of the sample ensures a constant O₂/N₂ ratio for air flowing into and out of the cold trap (Keeling et al., 1998). To prevent fractionation, we keep the flow of the air sample constant and use a 1/16 inch OD, 0.030 inch ID passivation-layer-coated Silcosteel® tubing (Restek Corp., Bellefonte, PA, USA) at the sample line where the temperature gradient exists. The dried sample is then introduced into the sample line of the O₂/N₂ ratio measurement system for analysis (see Tohjima (2000) for details of the measurement line).

2.2 Instruments and gas handling descriptions

Some components of the measurement system differ from those shown by Tohjima (2000). We use a GC-323(W) GC/TCD (GL Sciences Inc., Tokyo, Japan; hereinafter abbreviated as GC-323) as the detector instead of the Hewlett-Packard (HP) 5890

Detection of oxygen emission related to spring bloom

H. Yamagishi et al.

[Title Page](#)[Abstract](#)[Introduction](#)[Conclusions](#)[References](#)[Tables](#)[Figures](#)[◀](#)[▶](#)[◀](#)[▶](#)[Back](#)[Close](#)[Full Screen / Esc](#)[Printer-friendly Version](#)[Interactive Discussion](#)

GC/TCD to improve precision. Precision of the O_2/N_2 ratio is sensitive to temperature fluctuations of the separation column and the TCD detector (see Tohjima (2000) for details of the components in the measurement system). Thus, the heaters for the TCD and oven, as well as the fan in the GC oven, are turned off to prevent temperature fluctuations. Temperature fluctuations of the sample loop and the reference volumes for differential pressure sensors are also minimized by insulating them from room temperature. During the period of 17 March 2005–21 February 2006, analog output of the TCD has been digitized using a Hewlett-Packard 3396 Series II Integrator (USA). On 22 February 2006, the HP integrator was replaced by a 24-bit A/D converter (Chromato-
10 DAQ, Ulvac Inc., Chigasaki, Japan). Measurements, data acquisition, and calculation of peak area are performed using Visual Basic® (Microsoft Corp., Redmond, USA) since 22 February 2006.

In the GC/TCD, hydrogen gas (99.99999%) is used as the carrier gas, supplied by a Hydrogen Generator H2-300JA-100 (Perker Balston, Haverhill, USA). The carrier gas is introduced into the sample and reference cells of the TCD at a flow rate of 30 mL min^{-1} . Purified natural air in a 48-L aluminum cylinder compressed to a pressure of $\sim 8 \text{ MPa}$ is used as a reference gas. Concentrations of O_2 , N_2 , Ar, and CO_2 of the purified air are adjusted as required by adding O_2 , Ar, and CO_2 into the cylinder (Tohjima et al., 2008). Two reference gas cylinders are sent to the monitoring station once a year. These
20 cylinders are placed horizontally in heat-insulated wooden boxes to prevent thermal fractionation. Each cylinder is used as a working gas successively at a continuous flow rate of 8 mL min^{-1} . When the pressure of the cylinder being used decreases to $\sim 2 \text{ MPa}$, it is replaced with the second one. One cylinder lasts for more than 6 months.

Once a month, maintenance of the measurement system is carried out. During maintenance, two reference gas cylinders are compared to check stability of the O_2/N_2 ratio. The separation column is baked at 320°C for 300 min and the vapor traps are dried. The O_2/N_2 ratio of each reference gas cylinder is checked in our laboratory before and after each usage. We find that the O_2/N_2 ratio stays within 4 per meg before and after deployment at the monitoring station, indicating no significant drift.

The averaged O_2/N_2 ratio is, therefore, applied to the O_2/N_2 ratio of each reference gas cylinder.

2.3 Data processing

Changes of the O_2/N_2 ratio are expressed as relative deviations from a reference gas according to:

$$\delta(O_2/N_2) = \frac{(O_2/N_2)_S}{(O_2/N_2)_R} - 1, \quad (1)$$

where subscripts S and R denote sample and reference gases, respectively. Normally, the value of $\delta(O_2/N_2)$ is multiplied by 10^6 and expressed as per meg unit (Keeling and Shertz, 1992). The scale of the reference gas used in the present study is described elsewhere (Tohjima et al., 2008). The ratio of the (O_2+Ar) peak area to the N_2 peak area is directly determined by using the O_2/N_2 measurement system developed by Tohjima (2000). With the TCD sensitivity ratio of Ar relative to O_2 being expressed by k , the (O_2+Ar) peak area is related to the mole fractions of O_2 and Ar. One may define (Tohjima et al., 2000):

$$\delta\{(O_2 + Ar)/N_2\} = \frac{\{(X_{O_2} + kX_{Ar})/X_{N_2}\}_S}{\{(X_{O_2} + kX_{Ar})/X_{N_2}\}_R} - 1. \quad (2)$$

The value of k for HP5890 is slightly different from the one for GC-323 ($k_{HP}=1.13$ (Tohjima et al., 2005a) and $k_{GL}=1.08$, where the subscript symbols represent HP5890 and GC-323, respectively). Assuming that the value of $k(X_{Ar}/X_{N_2})_S - k(X_{Ar}/X_{N_2})_R$ is zero for any samples and reference gases (see Tohjima (2000) for details), $\delta(O_2/N_2)$ is related to $\delta\{(O_2+Ar)/N_2\}$:

$$\delta(O_2/N_2) = \delta\{(O_2 + Ar)/N_2\} \times \{(X_{O_2} + kX_{Ar})/X_{O_2}\}_R, \quad (3)$$

Detection of oxygen emission related to spring bloom

H. Yamagishi et al.

Title Page

Abstract

Introduction

Conclusions

References

Tables

Figures

◀

▶

◀

▶

Back

Close

Full Screen / Esc

Printer-friendly Version

Interactive Discussion

Detection of oxygen emission related to spring bloom

H. Yamagishi et al.

Title Page

Abstract

Introduction

Conclusions

References

Tables

Figures

◀

▶

◀

▶

Back

Close

Full Screen / Esc

Printer-friendly Version

Interactive Discussion

where $\{(X_{O_2} + kX_{Ar})/X_{O_2}\}_R$ is a scaling factor (1.050 for HP5890 (Tohjima et al., 2005a) and 1.048 for GC323). If the sample Ar/N₂ ratio increases by ~20 per meg, the O₂/N₂ ratio measured by the GC/TCD method is overestimated by ~1 per meg; this is based on the assumption of a constant Ar/N₂ ratio (definition of Ar/N₂ ratio is as follows:

5 $\delta(\text{Ar}/\text{N}_2) = \{(\text{Ar}/\text{N}_2)_{\text{sample}}/(\text{Ar}/\text{N}_2)_{\text{reference}} - 1\} \times 10^6$ (per meg)). This is a relatively valid assumption, since changes in the Ar/N₂ ratio are not likely to be significant in the present analysis of short-term variability in the O₂/N₂ ratio, because short term variability in the Ar/N₂ ratio is less than 30 per meg (see Battle et al., 2003; Blaine et al., 2006).

10 We found that the value of $\delta\{(O_2 + \text{Ar})/N_2\}$ measured by GC-323 ($\delta\{(O_2 + \text{Ar})/N_2\}_{\text{GL}}$) is not always equal to that measured by HP5890 GC/TCD ($\delta\{(O_2 + \text{Ar})/N_2\}_{\text{HP}}$) when we measure the same set of cylinders. The linearity of HP5890 GC/TCD was found to lie within ±1% based on the measurements of purified air gases that cover wide range of O₂/N₂ ratio (Tohjima et al., 2005a); the difference of $\delta\{(O_2 + \text{Ar})/N_2\}$ measured by two different types of TCD could be attributed to a nonlinear behavior of GC-323 GC/TCD

15 (see details in Sect. 2.3). The area ratio of $\delta\{(O_2 + \text{Ar})/N_2\}_{\text{GL}}$ is then corrected from the following equation:

$$\delta\{(O_2 + \text{Ar})/N_2\}_{\text{HP}} = \delta\{(O_2 + \text{Ar})/N_2\}_{\text{GL}}/L, \quad (4)$$

where L is the linearity correction factor for GC-323 ($L = 1.078 \pm 0.004$ at COI; Serial No. is GC-323-0338.). Note that the factor L is different for individual GC-323 GC/TCDs.

20 Slight difference in the value of the factor k (the TCD sensitivity ratio of Ar relative to O₂) between HP5890 and GC-323 can not explain the difference in the linearity of $\delta\{(O_2 + \text{Ar})/N_2\}$.

Here, APO is calculated by the following equation:

$$\delta\text{APO} = \delta(O_2/N_2)_{S/N} + \alpha_B X_{\text{CO}_2}/X_{O_2} - 1850 \text{ (per meg)}, \quad (5)$$

25 where X_{CO_2} is the CO₂ mol fraction in ppm, α_B is the O₂:C molar exchange ratio for the land biotic respiration and photosynthesis ($\alpha_B = 1.1$), X_{O_2} is the atmospheric O₂ mole fraction ($X_{O_2} = 0.2094$ (Tohjima et al., 2005a), and the value 1850 is the arbitrary APO

reference point (Tohjima et al., 2005b). We have calculated APO using in-situ CO₂ data obtained from the monitoring station (Mukai et al., 2001).

2.4 Linearity correction for TCD response

To estimate the linearity correction factor for the in-situ measurement system, we selected two 10L-aluminum cylinders of the purified air that is synthesized gravimetrically by Tohjima et al. (2005a). High and low O₂/N₂ ratio values of the two gravimetric standards cover the range of the variation of O₂/N₂ ratio observed at COI. Before and after calibration experiments, the ratios of $\delta\{(O_2+Ar)/N_2\}_{HP}$ in gravimetric standards were estimated in our laboratory using an HP 5890 GC/TCD. After relocation to the monitoring station, the two cylinders of the gravimetric standards were heat-insulated and kept horizontal for a month. The gravimetric standards were then measured as a sample gas relative to the working gas using a GC-323 GC/TCD in February and March 2007. We calculated the values of $\delta\{(O_2+Ar)/N_2\}_{GL}$ between gravimetric standards and estimated the linearity correction factor for each experiment (see Table 1). The linearity correction factor remained relatively constant for a month between the before- and after-calibration experiments (see Table 1). In our laboratory, we also examined the linearity of another GC-323 GC/TCD by measuring cylinders and samples for more than two years. The linear correlation between $\delta\{(O_2+Ar)/N_2\}_{HP}$ and $\delta\{(O_2+Ar)/N_2\}_{GL}$ stays within a range of ~2000 per meg and the slope of the correlation does not change significantly during the periods. Considering these results, we have adopted a constant value of 1.078 ± 0.004 for the linearity correction factor for the in-situ measurement system at COI (Table 1).

Although we have not yet identified the cause of the non-linearity inherent in GC-323, the difference in the linearity between these two instruments might be related to the difference in the physical structure between GC-323 and HP 5890 TCDs. Basically, TCD consists of four filaments in a Wheatstone bridge configuration. In GC-323, two filaments are exposed to the reference gas, and the other two filaments are exposed to the sample gas. In contrast, in the HP5890 detector only one TCD filament is exposed

Detection of oxygen emission related to spring bloom

H. Yamagishi et al.

Title Page

Abstract

Introduction

Conclusions

References

Tables

Figures

◀

▶

◀

▶

Back

Close

Full Screen / Esc

Printer-friendly Version

Interactive Discussion

alternately to the reference and sample gases very rapidly.

3 Results and discussion

3.1 Precision and data evaluation

The in-situ O_2/N_2 ratio and CO_2 concentration measurements from March 2005 to March 2006 are shown in Fig. 2a and APO is shown in Fig. 2b. The standard deviation of the O_2/N_2 ratio was estimated at $\sim\pm 14$ per meg (1σ) for half a day measurements when intra-hourly room temperature fluctuation was $0.5\text{--}1^\circ\text{C}$. Thus, standard error (SE) for 1-h mean O_2/N_2 ratio was $\sim\pm 6$ per meg (1.2 ppm). During August 2005 and from December 2005 to May 2006, the standard deviation of the O_2/N_2 ratio increased to 20–30 per meg because the range of room temperature fluctuation increased to $\sim 2^\circ\text{C}$. To reduce the influence of the room temperature fluctuation on the measurement precision, on 24 May 2006 GC/TCD and the sample loop were heat-insulated in an aluminum box, with the space between the inside and the outside plates of the box filled with water. This resulted in a stabilization of the O_2/N_2 ratio with a standard deviation of $\sim\pm 14$ per meg.

The in-situ O_2/N_2 ratio values were compared with those obtained from flask samples. As shown in Fig. 3a, there is a linear correlation between $\delta(O_2/N_2)$ from the flask sampling, $\delta(O_2/N_2)_{\text{flask}}$, and the in-situ 5-h mean O_2/N_2 ratio, $\delta(O_2/N_2)_{5\text{h}}$. The difference between $\delta(O_2/N_2)_{5\text{h}}$ and $\delta(O_2/N_2)_{\text{flask}}$ (denoted as $\Delta\delta(O_2/N_2)_{5\text{h}/\text{flask}}$) during March 2005–March 2006 is shown in Fig. 3b. The value of $\Delta\delta(O_2/N_2)_{5\text{h}/\text{flask}}$ was estimated to be 7.0 ± 9.9 per meg (1σ , $n=79$), whereas the difference between the in-situ 1-h mean O_2/N_2 ratio and the ratio from the flask measurements ($\Delta\delta(O_2/N_2)_{1\text{h}/\text{flask}}$) was found to be 8.4 ± 12.7 per meg (1σ , $n=79$).

Although we have not yet clearly identified the cause of the difference noted above, it is likely that a positive fractionation of O_2 relative to N_2 occurring in the sampling line is caused by the back pressure regulator (BPR) that adjusts the pressure of the spherical

Detection of oxygen emission related to spring bloom

H. Yamagishi et al.

Title Page

Abstract

Introduction

Conclusions

References

Tables

Figures

◀

▶

◀

▶

Back

Close

Full Screen / Esc

Printer-friendly Version

Interactive Discussion

Detection of oxygen emission related to spring bloom

H. Yamagishi et al.

Title Page

Abstract

Introduction

Conclusions

References

Tables

Figures

◀

▶

◀

▶

Back

Close

Full Screen / Esc

Printer-friendly Version

Interactive Discussion

flask (Fig. 1). Stephens et al. (2003) reported a fractionation of O_2 relative to N_2 by as much as 70 per meg when air sample flowing at a rate of 80 mL min^{-1} was separated from the main sample flow (6 L min^{-1}) by the tee junction located just before the BPR. In order to reduce the fractionation, they installed a 2 m of $1/4''$ tubing before the BPR and reduced the main flow rate to 2 L min^{-1} . In our system, air sample is allowed to flow for about 30 cm in a stainless steel tubing ($1/4''$ OD, 4.35 mm ID) from the spherical flask to the BPR at a rate of $\sim 8 \text{ L min}^{-1}$. The pressure and the flow rate govern the degree to which the fractionation occurs at BPR (Stephens et al., 2003); therefore, at the monitoring station, these were adjusted to 0.06 MPa and $\sim 8 \text{ L min}^{-1}$, respectively.

The standard deviation of $\Delta\delta(O_2/N_2)_{1 \text{ h/flask}}$ (± 12.7 per meg) is larger than the expected standard error (SE) of $\pm \sim 8$ per meg based on the SE of individual measurements from flasks ($SE = \pm 5$ per meg) and in-situ measurements ($SE = \pm 6$ per meg for 1-h mean O_2/N_2 ratio). The reasons for this could be due to the following factors: (1) Increase in the fluctuation of the room temperature during August 2005 and from December 2005 to May 2006 may have increased the standard error of $\Delta\delta(O_2/N_2)_{1 \text{ h/flask}}$ by ~ 1 per meg, and (2) Changes in the cold trap temperature may have contributed to the fractionation of O_2 from N_2 as the air sample passed through the 80-mL glass trap. There are other possible factors, such as the temporal variability of the O_2/N_2 ratio of the working gas and the difference in the sampling time for flasks and in-situ measurements.

3.2 Atmospheric observation

The observed O_2/N_2 ratio shows a seasonal variation characterized by many short-term variations with time scales of several hours to several days (Fig. 2a); these fluctuations are not resolved by the flask measurements since the flask sampling was done every 4 days. The observed higher variability in the O_2/N_2 ratios (Fig. 2a), compared to the APO variability, suggests that the O_2/N_2 variation was caused mainly by exchange with the terrestrial biosphere. In contrast, during the period from April to July, APO showed a large variability. Especially in late May to early July 2005, APO values

were about 40 per meg higher than the APO values observed during the neighboring months.

On the other hand, APO had no significant variabilities from October 2005 to March 2006 (Fig. 2b). In fall and winter, mixed layer depth of the ocean increases because of the enhancement of ventilation and surface waters are mixed with subsurface waters, in which O_2 is undersaturated. A decrease in the temperature of surface waters results in an increase in O_2 solubility; the extent of undersaturation is enhanced. These factors should result in an uptake of atmospheric O_2 into the oceans in fall and winter in the North Pacific near COI. At Trinidad Hed, California ($41.05^\circ N$, $124.15^\circ W$), strong coastal upwelling events occur from March to October, which transport the low-oxygen subsurface waters to the surface layer. The observed short-term declines of APO lasting several days or weeks by tens to ~ 100 per meg, which should be attributed to the uptake of atmospheric O_2 into the low-oxygen sea waters (Lueker et al., 2003, 2004). However, such short-term negative spikes of APO were not observed in winter time (from December to February) at COI (Fig. 2b). Therefore, the O_2 uptake in the western North Pacific near COI does not likely produce large heterogeneity of the atmospheric O_2/N_2 ratio in winter time.

3.3 Oxygen emission related to spring bloom

We focus on the APO variation from April to July 2005 (Fig. 4b, d) and examine the reasons for the high APO values during this period. We relate the APO variation at COI to the correlative patterns of the air mass transport (obtained through a back trajectory analysis) and the distribution of monthly-averaged marine net primary production (NPP), as shown in Fig. 5. We have computed the back trajectories using the CGER/METEX trajectory model (Zeng et al., 2003) forced by a 3-d wind field on a sigma vertical coordinate; the altitude of the starting point is 500 m, integrating back for 120 h. Monthly NPP distribution is estimated from the Vertically Generalized Production Model (VGPM) (Behrenfeld and Falkowski, 1997), which is a widely used satellite-derived NPP estimation.

Detection of oxygen emission related to spring bloom

H. Yamagishi et al.

Title Page

Abstract

Introduction

Conclusions

References

Tables

Figures

◀

▶

◀

▶

Back

Close

Full Screen / Esc

Printer-friendly Version

Interactive Discussion

Detection of oxygen emission related to spring bloom

H. Yamagishi et al.

[Title Page](#)[Abstract](#)[Introduction](#)[Conclusions](#)[References](#)[Tables](#)[Figures](#)[⏪](#)[⏩](#)[◀](#)[▶](#)[Back](#)[Close](#)[Full Screen / Esc](#)[Printer-friendly Version](#)[Interactive Discussion](#)

Because of the relatively rapid air-sea exchange of oxygen, re-equilibration of O_2 in a mixed layer depth of 50 m occurs on a timescale of days (Gruber et al., 2001). Mixed layer depth is much less than 50 m (typically 5–30 m) during spring bloom in the Japan Sea (Jo et al., 2007) and the Okhotsk Sea (Okunishi et al., 2005), and is about 50 m in the western North Pacific (Imai et al., 2002). Therefore, the time lag between O_2 production and emission should be small (several days). In April 2005, the spring bloom occurred mainly in the Japan Sea and the region between $30^\circ N$ and $40^\circ N$ in the western North Pacific (Fig. 5a). High values of APO were observed at COI (red symbols from a1 to a5 in Fig. 4b) when the air mass trajectories passed over the high productive regions (Fig. 5a). On the other hand, low APO values were observed (blue symbols from b1 to b5 in Fig. 4b) when the air mass trajectories passed over the low productive regions (Fig. 5b). In June, high APO values (red symbols from c1 to c6 in Fig. 4d) were related to the strong bloom observed in the Okhotsk Sea and in the region $40\sim 50^\circ N$ in the western North Pacific (Fig. 5c), while low APO values (blue symbols from d1 to d4 in Fig. 4d) were related to air mass trajectories passing over the low productive regions (see Fig. 5d). Back trajectory analysis indicates that high values of APO are associated with air masses that have passed over the regions of active biological photosynthesis (spring bloom), showing that the O_2 emission related to marine primary production can be observed by in-situ monitoring of atmospheric O_2/N_2 ratio and CO_2 concentration.

Not all of the APO variability at COI, however, can be explained by the NPP-trajectory relationship. For example, a large increase in APO was observed on 3 June 2005 and an APO fluctuation on 24–27 June 2005. We are in the process of carrying out a detailed analysis of these events.

4 Summary and implications

We have been carrying out in-situ measurements of the atmospheric O_2/N_2 ratio at Cape Ochi-ishi (COI; $43^\circ 10' N$, $145^\circ 30' E$) in the northern part of Japan since March

Detection of oxygen emission related to spring bloom

H. Yamagishi et al.

2005 using the GC/TCD analyzer. The standard deviation of the O_2/N_2 ratio is estimated to be about ± 14 per meg (≈ 3 ppm) for the in-situ measurement system, resulting in a standard error of ± 6 per meg (≈ 1.2 ppm) for the 1-h mean O_2/N_2 ratio. Although precision of the GC/TCD method is worse than that of the other in-situ measurement systems, the smaller consumption rate of working gas (8 mL min^{-1}) is a benefit for long term observation at remote monitoring stations. After linearity correction in the in-situ measurement system, there remains a systematic bias for the O_2/N_2 ratio measured in situ compared with the O_2/N_2 ratio obtained from the flask measurements. The average of the differences between the in-situ and the flask measurements (5-h mean O_2/N_2 ratio – flask data) is 7.0 ± 9.9 per meg (1σ , $n=79$) from March 2005 to March 2006.

During the period of our study, we have observed a clear seasonal variation in APO at COI. From late May to early July 2005, APO shows relatively high values, exceeding the values observed during the neighboring months by about 40 per meg, and is characterized by a large variability. Based on the results from trajectory analysis, it is suggested that the high values of APO at COI are associated with occurrences of strong marine primary production (spring bloom) observed in the Okhotsk Sea and the western North Pacific. This gives additional support to the idea that the variation in APO reflects variation in O_2 emission associated with the spring bloom of phytoplankton in the western North Pacific and marginal seas near Japan.

Acknowledgements. We are thankful to F. Shimano, H. Sakai, K. Sengoku, and N. Oda for maintenance of our in-situ measurement system. We thank S. Hashimoto for processing CO_2 data and A. Watanabe for writing software programs for measurement. We thank J. Zeng for providing back trajectory analysis tools. We also thank S. Maksyutov, Y. Koyama, Y. Yamanaka, H. Tanimoto, T. Machida, K. Shimoyama, and T. Saino for valuable discussions. Monitoring station is maintained by the Center for Global Environmental Research (CGER) and Global Environmental Forum (GEF). This work was supported by the Global Environment Research Coordination System of the Ministry of the Environment, Japan and partly supported by the Grants-in-Aid for Creative Scientific Research (2005/17GS0203) of the Ministry of Education, Science, Sports and Culture, Japan.

Title Page

Abstract

Introduction

Conclusions

References

Tables

Figures

◀

▶

◀

▶

Back

Close

Full Screen / Esc

Printer-friendly Version

Interactive Discussion

References

- Balkanski, Y., Monfray, P., Battle, M., and Heimann, M.: Ocean primary production derived from satellite data: An evaluation with atmospheric oxygen measurements, *Global Biogeochem. Cy.*, 13(2), 257–271, 1999.
- 5 Battle, M., Bender, M., Hendricks, M. B., Ho, D. T., Mika, R., McKinley, G., Fan, S. M., Blaine, T., and Keeling, R. F.: Measurements and models of the atmospheric Ar/N₂ ratio, *Geophys. Res. Lett.*, 30(15), 1786, doi:10.1029/2003GL017411, 2003.
- Battle, M., Fletcher, S. M., Bender, M. L., Keeling, R. F., Manning, A. C., Gruber, N., Tans, P. P., Hendricks, M. B., Ho, D. T., Simonds, C., Mika, R., and Paplawsky, B.: Atmospheric potential
10 oxygen: New observations and their implications for some atmospheric and oceanic models, *Global Biogeochem. Cy.*, 20(1), GB1010, doi: 10.1029/2005GB002534, 2006.
- Behrenfeld, M. J. and Falkowski, P. G.: Photosynthetic rates derived from satellite-based chlorophyll concentration, *Limnol. Oceanogr.*, 42(1), 1–20, 1997.
- Bender, M., Ellis, T., Tans, P., Francey, R., and Lowe, D.: Variability in the O₂/N₂ ratio of southern hemisphere air, 1991-1994: Implications for the carbon cycle, *Global Biogeochem. Cy.*,
15 10(1), 9–21, 1996.
- Bender, M. L., Tans, P. P., Ellis, J. T., Orchardo, J., and Habfast, K.: A high-precision isotope ratio mass-spectrometry method for measuring the O₂/N₂ ratio of air, *Geochim. Cosmochim. Ac.*, 58(21), 4751–4758, 1994.
- 20 Blaine, T. W., Keeling, R. F., and Paplawsky, W. J.: An improved inlet for precisely measuring the atmospheric Ar/N₂ ratio, *Atmos. Chem. Phys.*, 6, 1181–1184, 2006,
<http://www.atmos-chem-phys.net/6/1181/2006/>.
- Broecker, W. S. and Peng, T.-H.: *Tracers in the Sea*, Eldigio Press, New York, 1982.
- Gruber, N., Gloor, M., Fan, S. M., and Sarmiento, J. L.: Air-sea flux of oxygen estimated from
25 bulk data: Implications for the marine and atmospheric oxygen cycles, *Acta*, 15(4), 783–803, 2001.
- He, M. X., Liu, Z. S., Du, K. P., Li, L. P., Chen, R., Carder, K. L., and Lee, Z. P.: Retrieval of chlorophyll from remote-sensing reflectance in the China seas, *Appl. Opt.*, 39(15), 2467–2474, 2000.
- 30 Imai, K., Nojiri, Y., Tsurushima, N., and Saino, T.: Time series of seasonal variation of primary productivity at station KNOT (44 degrees N, 155 degrees E) in the sub-arctic western North Pacific, *Deep-Sea Res. Pt. II*, 49(24–25), 5395–5408, 2002.

ACPD

8, 2225–2248, 2008

Detection of oxygen emission related to spring bloom

H. Yamagishi et al.

Title Page

Abstract

Introduction

Conclusions

References

Tables

Figures

◀

▶

◀

▶

Back

Close

Full Screen / Esc

Printer-friendly Version

Interactive Discussion

EGU

Jo, C. O., Lee, J. Y., Park, K. A., Kim, Y. H., and Kim, K. R.: Asian dust initiated early spring bloom in the northern East/Japan Sea, *Geophys. Res. Lett.*, 34(5), L05602, doi:10.1029/2006GL027395, 2007.

Keeling, R. F.: Development of an interferometric oxygen analyzer for precise measurements of the atmospheric O₂ mole fraction., PhD thesis, Harvard University, 1988.

Keeling, R. F. and Shertz, S. R.: Seasonal and Interannual Variations in Atmospheric Oxygen and Implications for the Global Carbon-Cycle, *Nature*, 358(6389), 723–727, 1992.

Keeling, R. F., Manning, A. C., McEvoy, E. M., and Shertz, S. R.: Methods for measuring changes in atmospheric O₂ concentration and their application in southern hemisphere air, *J. Geophys. Res.-Atmos.*, 103(D3), 3381–3397, 1998.

Keeling, R. F., Blaine, T., Paplawsky, B., Katz, L., Atwood, C., and Brockwell, T.: Measurement of changes in atmospheric Ar/N₂ ratio using a rapid-switching, single-capillary mass spectrometer system, *Tellus B*, 56(4), 322–338, 2004.

Lueker, T. J., Walker, S. J., Vollmer, M. K., Keeling, R. F., Nevison, C. D., Weiss, R. F., and Garcia, H. E.: Coastal upwelling air-sea fluxes revealed in atmospheric observations of O₂/N₂, CO₂ and N₂O, *Geophys. Res. Lett.*, 30(6), 1292, doi: 10.1029/2002GL016615, 2003.

Lueker, T. J.: Coastal upwelling fluxes of O₂, N₂O, and CO₂ assessed from continuous atmospheric observations at Trinidad, California, *Biogeosciences*, 1(1), 101–111, 2004.

Manning, A. C., Keeling, R. F., and Severinghaus, J. P.: Precise atmospheric oxygen measurements with a paramagnetic oxygen analyzer, *Global Biogeochem. Cy.*, 13(4), 1107–1115, 1999.

Manning, A. C.: Temporal variability of atmospheric oxygen from both continuous measurements and flask sampling network: Tools for studying the global carbon cycle, PhD thesis, University of California, San Diego, 2001.

Manning, A. C. and Keeling, R. F.: Global oceanic and land biotic carbon sinks from the Scripps atmospheric oxygen flask sampling network, *Tellus B*, 58(2), 95–116, 2006.

Mukai, H., Katsumoto, M., Ide, R., Machida, T., Fujinuma, Y., Nojiri, Y., Inagaki, M., Oda, N., and Watai, T.: Characterization of atmospheric CO₂ observed at two-background air monitoring stations (Hateruma and Ochi-ishi) in Japan, in Sixth International Carbon Dioxide Conference, Extended Abstract, Vol. I, edited by Tohoku University, 108–111, Sendai, Japan, 2001.

Okunishi, T., Kishi, M. J., Shiimoto, A., Tanaka, H., and Yamashita, T.: An ecosystem modeling study of spatio-temporal variations of phytoplankton distribution in the Okhotsk Sea,

Detection of oxygen emission related to spring bloomH. Yamagishi et al.

Title Page

Abstract

Introduction

Conclusions

References

Tables

Figures

◀

▶

◀

▶

Back

Close

Full Screen / Esc

Printer-friendly Version

Interactive Discussion

Detection of oxygen emission related to spring bloom

H. Yamagishi et al.

Title Page

Abstract

Introduction

Conclusions

References

Tables

Figures

◀

▶

◀

▶

Back

Close

Full Screen / Esc

Printer-friendly Version

Interactive Discussion

Continental Shelf Research, 25(12–13), 1605–1628, 2005.

Severinghaus, J. P.: Studies of the terrestrial O₂ and carbon cycles in sand dune gases and in Biosphere 2., PhD thesis, Columbia Univ., 1995.

Stephens, B. B., Keeling, R. F., Heimann, M., Six, K. D., Murnane, R., and Caldeira, K.: Testing global ocean carbon cycle models using measurements of atmospheric O₂ and CO₂ concentration, *Global Biogeochem. Cy.*, 12(2), 213–230, 1998.

Stephens, B. B.: Field-based Atmospheric Oxygen Measurements and the Ocean Cycle, Ph. D. thesis, Scripps Institution of Oceanography, Univ. of Calif., San Diego, 1999.

Stephens, B. B., Keeling, R. F., and Paplawsky, W. J.: Shipboard measurements of atmospheric oxygen using a vacuum-ultraviolet absorption technique, *Tellus B*, 55(4), 857–878, 2003.

Stephens, B. B., Bakwin, P. S., Tans, P. P., Teclaw, R. M., and Baumann, D. D.: Application of a differential fuel-cell analyzer for measuring atmospheric oxygen variations, *J. Atmos. Ocean. Tech.*, 24(1), 82–94, 2007.

Sturm, P., Leuenberger, M., Valentino, F. L., Lehmann, B., and Ihly, B.: Measurements of CO₂, its stable isotopes, O₂/N₂, and ²²²Rn at Bern, Switzerland, *Atmos. Chem. Phys.*, 6, 1991–2004, 2006,

<http://www.atmos-chem-phys.net/6/1991/2006/>.

Tohjima, Y.: Method for measuring changes in the atmospheric O₂/N₂ ratio by a gas chromatograph equipped with a thermal conductivity detector, *J. Geophys. Res.-Atmos.*, 105(D11), 14 575–14 584, 2000.

Tohjima, Y., Mukai, H., Machida, T., and Nojiri, Y.: Gas-chromatographic measurements of the atmospheric oxygen/nitrogen ratio at Hateruma Island and Cape Ochi-ishi, Japan, *Geophys. Res. Lett.*, 30(12), 1653, doi:10.1029/2003GL017282, 2003.

Tohjima, Y., Mukai, H., Nojiri, Y., Yamagishi, H., and Machida, T.: Atmospheric O₂/N₂ measurements at two Japanese sites: estimation of global oceanic and land biotic carbon sinks and analysis of the variations in atmospheric potential oxygen (APO), *Tellus B, OnlineEarly Articles*, doi:10.1111/j.1600-0889.2007.00334.x., 2008.

Tohjima, Y., Machida, T., Watai, T., Akama, I., Amari, T., and Moriwaki, Y.: Preparation of gravimetric standards for measurements of atmospheric oxygen and reevaluation of atmospheric oxygen concentration, *J. Geophys. Res.-Atmos.*, 110, D11302, doi:10.1029/2004JD005595, 2005a.

Tohjima, Y., Mukai, H., Machida, T., Nojiri, Y., and Gloor, M.: First measurements of the latitudinal atmospheric O₂ and CO₂ distributions across the western Pacific, *Geophys. Res. Lett.*,

32, L17805, doi:10.1029/2005GL023311, 2005b.

Zeng, J., Katsumoto, M., Ide, R., Inagaki, M., Mukai, H., and Fujinuma, Y.: Development of meteorological data explorer for Windows., in Data Analysis and Graphic Display System for Atmospheric Research using PC, CGER-M014-2003, edited by Fujinuma, Y., 19–73, Center for Global Environmental Research / NIES, Tsukuba, 2003.

5

ACPD

8, 2225–2248, 2008

Detection of oxygen emission related to spring bloom

H. Yamagishi et al.

Title Page

Abstract

Introduction

Conclusions

References

Tables

Figures

⏪

⏩

◀

▶

Back

Close

Full Screen / Esc

Printer-friendly Version

Interactive Discussion

EGU

Detection of oxygen emission related to spring bloom

H. Yamagishi et al.

Table 1. Results of linearity calibration experiments.

GC/TCD	$\delta\{(O_2+Ar)/N_2\}_{S1/S2}$ (per meg) ^a	Linearity correction factor, L	Date of experiments
HP5890	491.3±1.4	–	–
GC-323	529.7±1.9	1.078±0.005	19–20 Feb. 2007
GC-323	529.3±1.8	1.077±0.005	18–19 March 2007
GC-323 (average)	–	1.078±0.004	–

^a Symbols of S1 and S2 represent cylinders of CPB-26855 and CPB-17279, respectively. Values of $\delta\{(O_2+Ar)/N_2\}_{HP}$ of the cylinders S1 and S2 were estimated at 63.3±1.0 and –428.0±1.0 per meg, respectively. Value of $\delta\{(O_2+Ar)/N_2\}_{S1/S2}$ represents $\delta\{(O_2+Ar)/N_2\}$ of the cylinder S1 relative to that of S2.

Title Page

Abstract

Introduction

Conclusions

References

Tables

Figures

◀

▶

◀

▶

Back

Close

Full Screen / Esc

Printer-friendly Version

Interactive Discussion

Detection of oxygen emission related to spring bloom

H. Yamagishi et al.

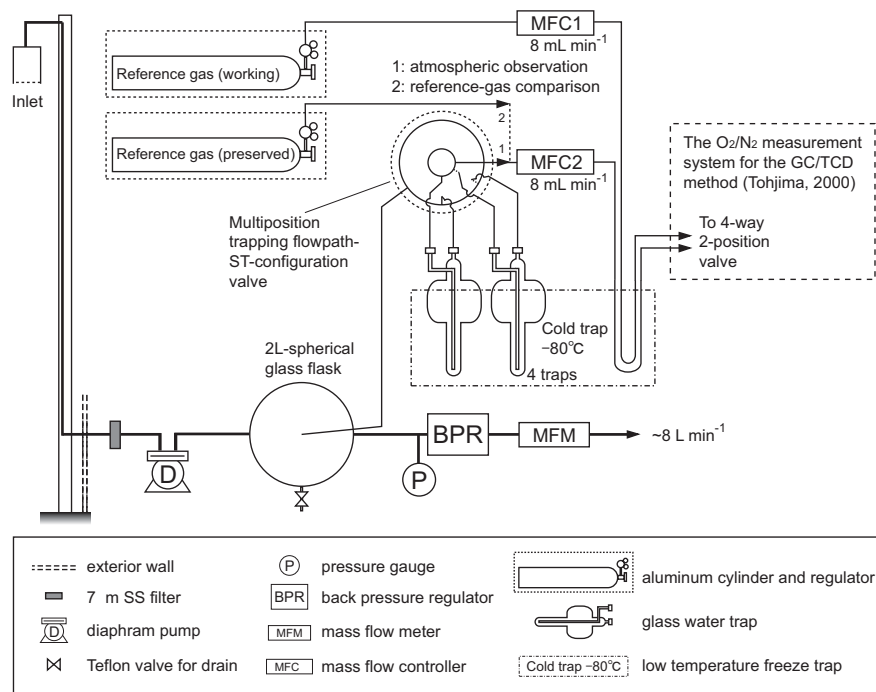


Fig. 1. Schematic diagram of the sampling line for the in-situ O_2/N_2 measurement system using the GC/TCD method developed by Tohjima (2000).

Title Page

Abstract

Introduction

Conclusions

References

Tables

Figures

◀

▶

◀

▶

Back

Close

Full Screen / Esc

Printer-friendly Version

Interactive Discussion

Detection of oxygen emission related to spring bloom

H. Yamagishi et al.

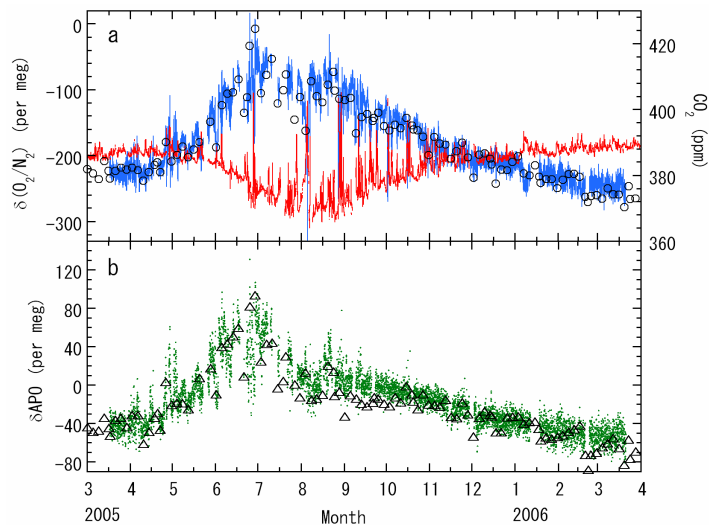


Fig. 2. One-hour mean O_2/N_2 ratio (blue line,(a)), CO_2 concentration (red line, a), and δAPO (green dot,(b)) measured in situ at Cape Ochi-ishi from March 2005 to March 2006. Open circles (a) and open triangles (b) represent O_2/N_2 ratio and δAPO , respectively, of flask samples.

[Title Page](#)[Abstract](#)[Introduction](#)[Conclusions](#)[References](#)[Tables](#)[Figures](#)[◀](#)[▶](#)[◀](#)[▶](#)[Back](#)[Close](#)[Full Screen / Esc](#)[Printer-friendly Version](#)[Interactive Discussion](#)

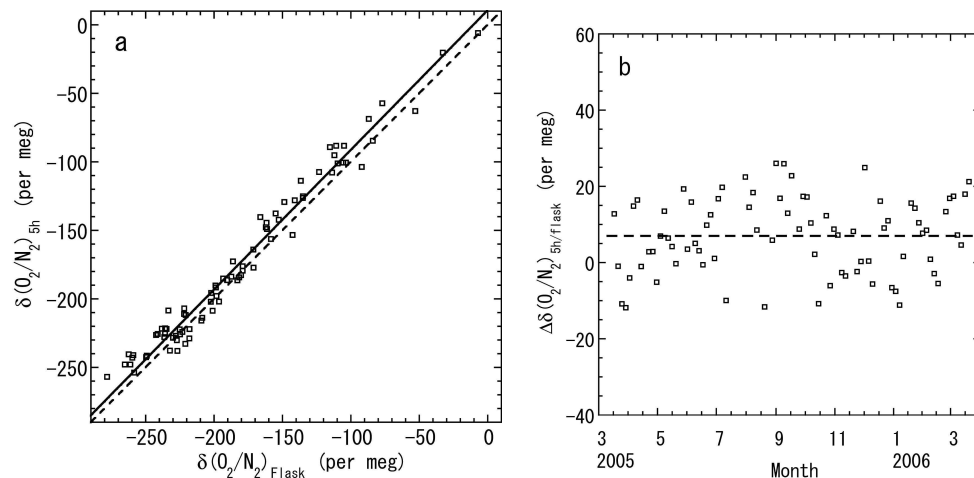


Fig. 3. Comparison of $\delta(\text{O}_2/\text{N}_2)$ between the flask, $\delta(\text{O}_2/\text{N}_2)_{\text{flask}}$, and the 5-h mean in-situ O_2/N_2 ratio, $\delta(\text{O}_2/\text{N}_2)_{5\text{h}}$, from 17 February 2005 to 20 March 2006. **(a)** Solid and broken lines are the reduced measure axis regression ($Y=1.02X+10.5$) and the function of $Y=X$, respectively. Plot represents the 5-h mean $\delta(\text{O}_2/\text{N}_2)$ measured in situ. **(b)** Deviation of the in-situ measurements from the flask measurements (i.e. $\Delta\delta(\text{O}_2/\text{N}_2)_{5\text{h}/\text{flask}} = \delta(\text{O}_2/\text{N}_2)_{5\text{h}} - \delta(\text{O}_2/\text{N}_2)_{\text{flask}}$). Broken line represents $Y=7.0$, which is an average of the deviation.

Detection of oxygen emission related to spring bloom

H. Yamagishi et al.

Title Page

Abstract

Introduction

Conclusions

References

Tables

Figures

◀

▶

◀

▶

Back

Close

Full Screen / Esc

Printer-friendly Version

Interactive Discussion

Detection of oxygen emission related to spring bloom

H. Yamagishi et al.

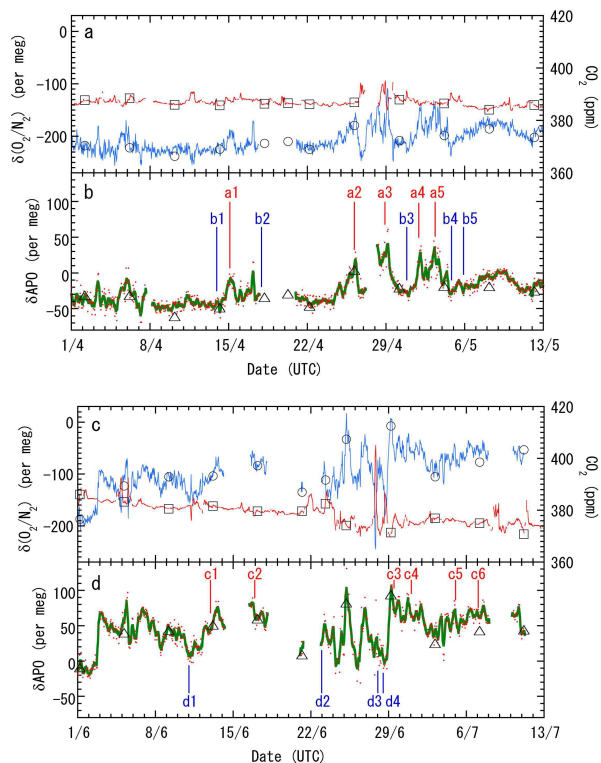


Fig. 4. One-hour mean O_2/N_2 ratio, CO_2 mole fraction, and δAPO at Cape Ochi-ishi for the periods of 1 April–12 May (**a, b**) and 1 July–12 July (**c, d**) in 2005. One-hour mean O_2/N_2 ratio (blue lines in **a** and **c**), CO_2 mole fraction (red lines in **a** and **c**), and δAPO (red dots in **b** and **d**), and 5-h running mean δAPO (green lines in **b** and **d**) are shown. Dots represent the O_2/N_2 ratio (open circles in **a** and **c**), CO_2 mole fraction (open squares in **a** and **c**), and δAPO (open triangles in **b** and **d**) of the flask samples. Times indicated by **a1** to **d4** in pointing δAPO (in **b** and **d**) represent the starting times of the back trajectory calculations shown in Fig. 5a–d (see Sect. 3.3 for details). The numbers from 1 to 6 are comparable with those in the legends of Fig. 5.

[Title Page](#)
[Abstract](#)
[Introduction](#)
[Conclusions](#)
[References](#)
[Tables](#)
[Figures](#)
[◀](#)
[▶](#)
[◀](#)
[▶](#)
[Back](#)
[Close](#)
[Full Screen / Esc](#)
[Printer-friendly Version](#)
[Interactive Discussion](#)

Detection of oxygen emission related to spring bloom

H. Yamagishi et al.

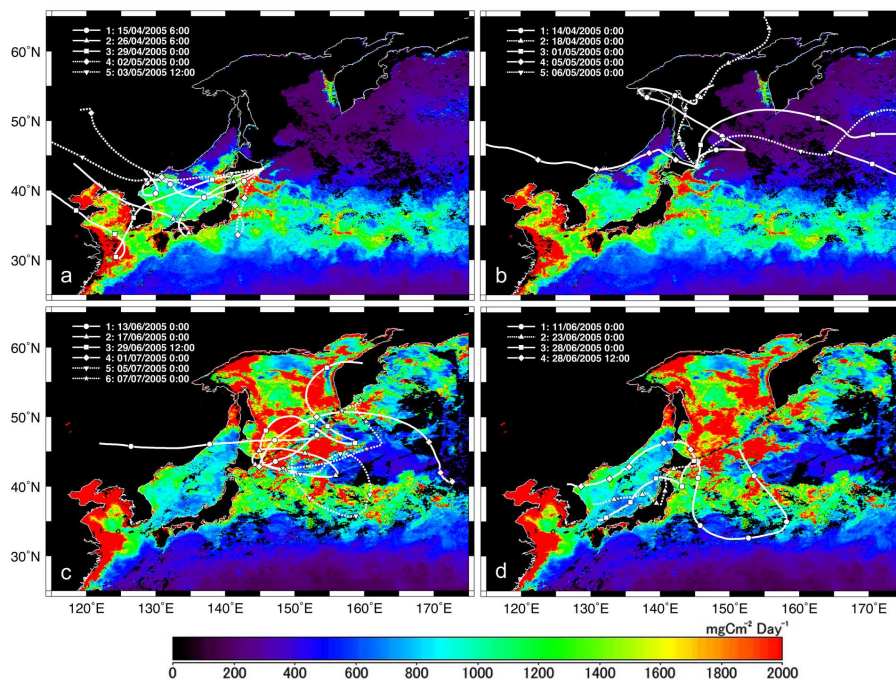


Fig. 5. Monthly-average distribution of the net primary production in April (**a**, **b**) and June (**c**, **d**) 2005 estimated from the Vertically Generalized Production Model (VGPM) (Behrenfeld and Falkowski, 1997), along with 5-day air mass back trajectories. The NPP estimation in the East China Sea and Yellow Sea might be overestimated due to suspended matter and chromophoric dissolved organic matter (He et al., 2000). Legends show the start time (UTC) for calculating back trajectories.

Title Page

Abstract

Introduction

Conclusions

References

Tables

Figures

◀

▶

◀

▶

Back

Close

Full Screen / Esc

Printer-friendly Version

Interactive Discussion